ANALYSIS OF NONLINEAR BEAM-COLUMNS

by

Ronald Boyd Shiflett

Thesis submitted to the Graduate Faculty of the

Virginia Polytechnic Institute and State University

in partial fulfillment of the requirements for the degree of

MASTER OF SCIENCE

in

Civil Engineering

APPROVED:

S. M. Holzer, Chairman

C. S. Desai

A. E. Somers, Jr.

April 1977
Blacksburg, Virginia

ACKNOWLEDGEMENTS

I acknowledge and thank Dr. Siegfried M. Holzer for his suggestions and ideas, which were fundamental to my understanding of the model, and for his help in editing the manuscript. Also, my thanks are extended to Dr. A.E. Somers, Ayodele Abatan, and Kamol Wongkoltoot for their ideas during the research for this report. Indispensable to the preparation of the manuscript are Audrey L. Shiflett and Juanita C. Lilly.

TABLE OF CONTENTS

TABLE OF CONTENTS

(continued)

LIST OF FIGURES

LIST OF TABLES

CHAPTER I

INTRODUCTION

A one dimensional finite element model has been developed and used by Holzer, et al, [2] to simulate the behavior of inelastic, geometrically nonlinear beam-columns. Bradshaw [1] has written a computer code to study some of the characteristics of this model. Specifically, the geometrically nonlinear, elastic response predictions were investigated. The formulation contained in Bradshaw's computer code is the basis for this thesis.

The work done by this writer was to incorporate a bilinear inelastic constitutive law into the model. An investigation was conducted to test the performance of the inelastic model.

The remainder of Chapter One highlights the fundamental features of the elastic model [1]. In Chapter Two the formulation which is necessary to achieve the modeling of inelastic material behavior is presented. Demonstration problems used to test the inelastic model are described in Chapter Three. In Chapter Four, suggestions are outlined which may enhance the use of this model and its capabilities are discussed.

Notes On The Mathematical Model

The model studied by Bradshaw [1] is a finite element model. A plane frame structure is idealized by an assemblage of one-dimensional beam-column elements.

Element Model

The deformed element reference axis, defined by displacements u(x) and v(x), is shown in Fig. 1. Geometric nonlinearity is introduced into the element model by coupling axial and flexural internal distortions.

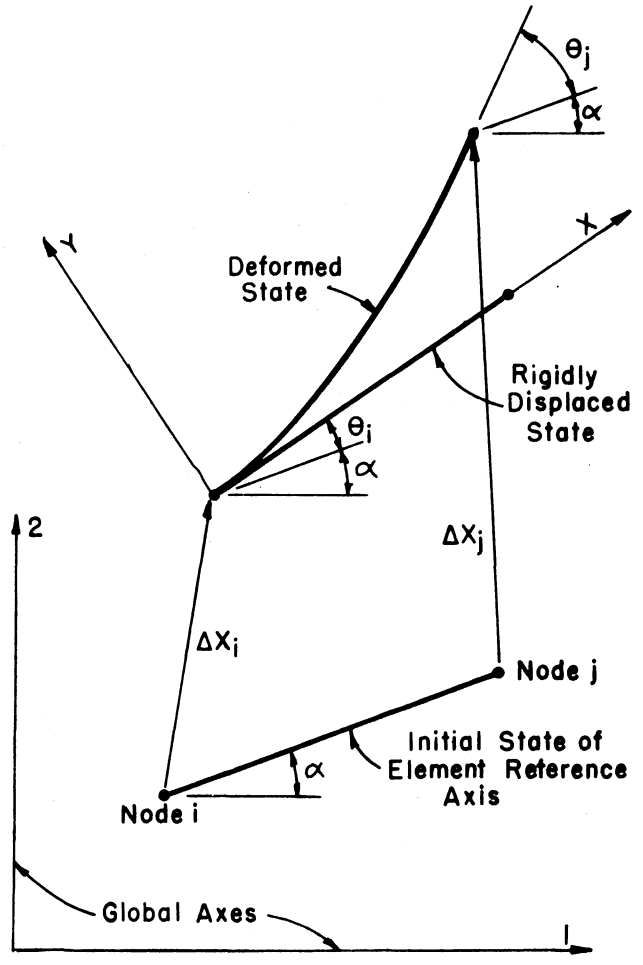

ΔX_i and ΔX_j Are Translational Displacements of Nodes i and j
θ_i and θ_j Are Rotational Displacements of Nodes i and j

ELEMENT REFERENCE AXIS

FIGURE 1 – ELEMENT DISPLACEMENT MODEL

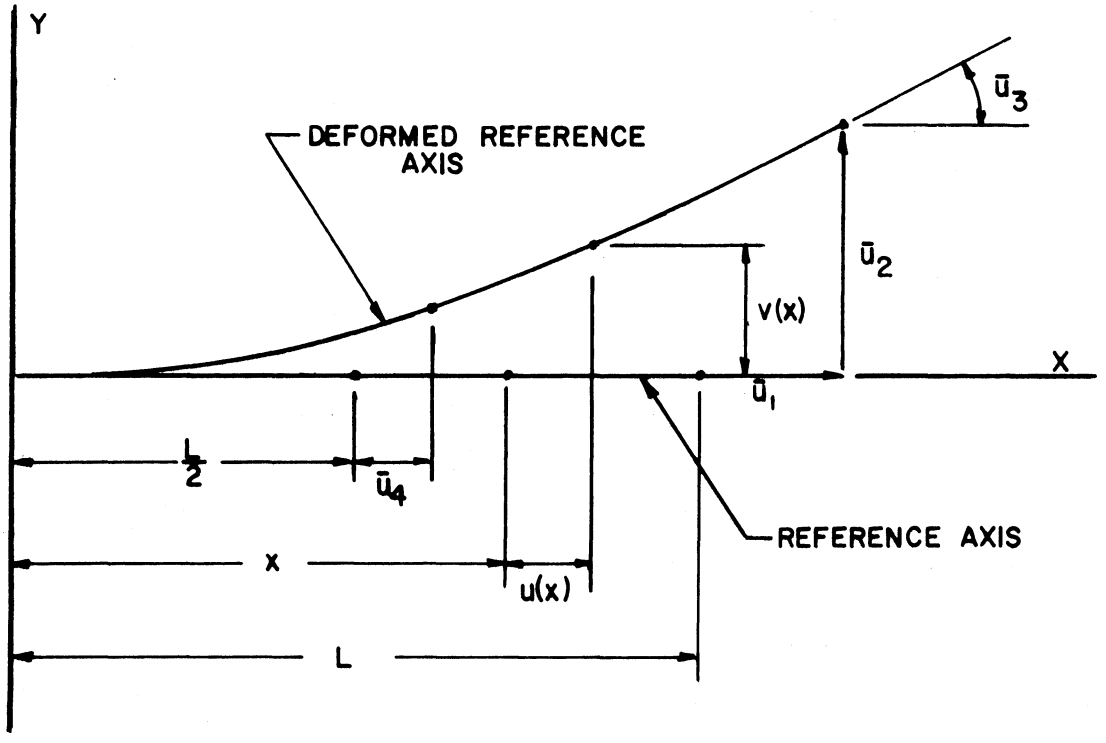

DISTORTION COMPONENTS

FIGURE 1 – ELEMENT DISPLACEMENT MODEL CONTINUED

This is done by including a nonlinear term [$1/2(dv/dx)^2$] in the strain-displacement relation [2].

In order that the internal energy of an element may be evaluated, a measure of distortion of the element is needed with all rigid body motion eliminated. This is accomplished with a set of parameters called distortion components ($\bar{u}_1$, $\bar{u}_2$, $\bar{u}_3$, $\bar{u}_4$). The distortion components are illustrated in Fig. 1. Components $\bar{u}_1$, $\bar{u}_2$, and $\bar{u}_3$ are obtained from global nodal displacements. Component $\bar{u}_4$ is prescribed during the solution process [2].

The magnitudes of the distortion components are restricted only by the limitation that strains must be small [2].

Element internal energy for nonlinearly elastic material behavior is computed by numerically integrating the strain energy density over the domain of the element. This is done via the Gaussian quadrature [3]. During the summation of the Gaussian quadrature, the strain energy density must be computed at discrete points in the domain of the element. These Gauss points are determined by the quadrature algorithm according to the number of points judged necessary by the model user. The user must prescribe the number of points parallel to and perpendicular to the element reference axis. Together, these two numbers are known as the Gauss rule of the Gauss point distribution. Fig. 2 illustrates the distribution of points for 2 X 2 and 5 X 3 Gauss rules.

System Model

All information about the deformed state of the system is contained in an energy function which is the total potential energy of the system. This energy function is defined by the nodal displacements which are the

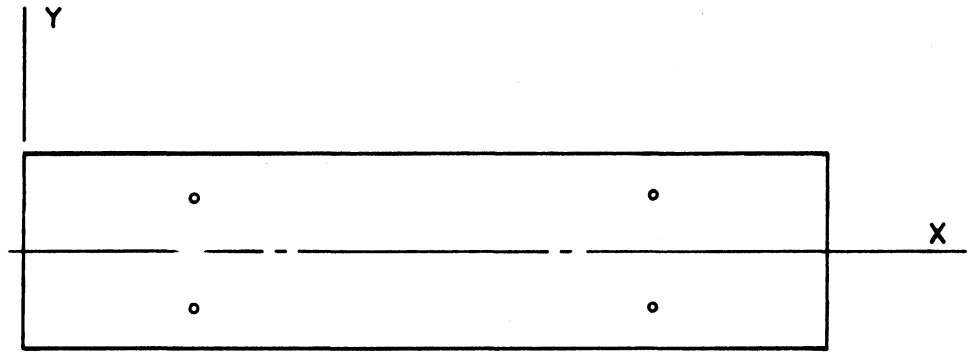

2 x 2 GAUSS RULE

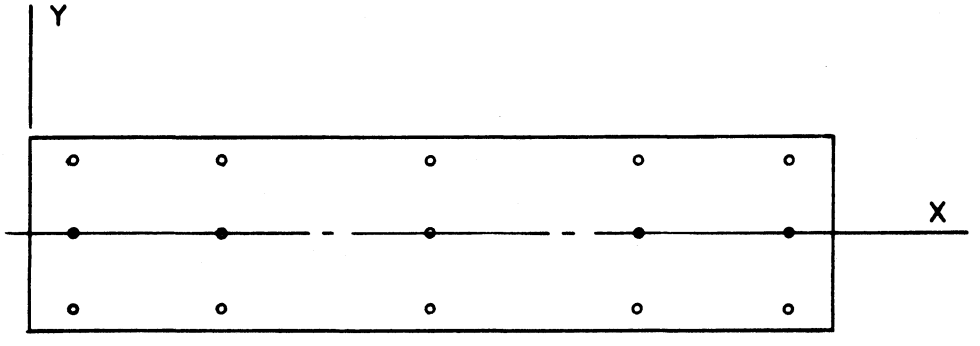

5 x 3 GAUSS RULE

FIGURE 2 – EXAMPLES OF GAUSS POINT DISTRIBUTION

generalized coordinates of the finite element model [2].

Compatibility is accomplished by formulating the distortion components in terms of the nodal displacements [2].

A configuration of nodal displacements which is in equilibrium with a given set of loads is achieved by minimizing the system energy.

Solution Process

The equilibrium configuration corresponding to a set of external forces is produced by repetitively "guessing" a displacement configuration, computing the energy function, and examining the magnitude of the gradients to the function until a minimal value is found. This is accomplished via an iterative solution process which incorporates a minimization algorithm [1]. The basic method contained in the algorithm is discussed by Fletcher and Powell [9].

The analysis of displacement behavior of a beam-column system proceeds by determining a set of nodal displacements, and equilibrium configuration, for each set of nodal loads. Each set of nodal loads is called a load configuration. Typically, displacement configurations are desired for a set of load configurations representing some scheme of adding or removing load from a structure. The set of increments or decrements of load corresponding to each degree of freedom which, when added to a load configuration yield the succeeding load configuration, is known as a load step. The set of displacement configurations corresponding to a set of load configurations involved in an investigation represents discrete points on the equilibrium path.

As noted by Bradshaw [(1); p. 21], at the beginning of the solution for an equilibrium configuration, an initial guess of the magnitudes of

the nodal displacements must be provided for the minimization algorithm. When the investigation is started at the unstrained state of the system, the ititial guess consists of a vector of zeros, one for each degree of freedom. Frequently, an investigation begins at some known displacement configuration. In this case the initial guess is that initial configuration.

CHAPTER II

Internal Energy for Inelastic Material Behavior

Element and System Energies

The nonlinearly elastic model investigated by Bradshaw is conservative. Hence, the internal energy of an element is the strain energy of that element. Furthermore, the sum of all the element strain energies and the potential energies of the external forces constitute the total potential energy of the system.

In an inelastic system, a certain amount of energy is retained by the system after some or all of its components have been strained beyond the yield point and then unloaded. The internal energy of an element, m, and of the system are designated Π_m and Π, respectively. The sum of the system internal energy and the potential energy of the external forces is an energy function designated E; consequently,

$$E = \Pi + \Omega \qquad (1)$$

where Ω is the potential energy of the external forces [2]. This function, E, replaces the total potential energy function, V, used by Bradshaw [(1); p. 14] in the solution process.

The internal energy, Π, is computed by summing the internal energies of all elements in the system [(1); p. 14]. The internal energy of each element is computed by integrating numerically the internal energy density over the domain of the element using the Gaussian quadrature [(10) p. 14 eq. 24].

System Gradient

Part of the input information for the minimization routine is a vector

of gradients of the system internal energy function. These gradients are the partial derivatives of the system internal energy with respect to the generalized coordinates. Restating from Bradshaw [(1); p. 21], the contribution to the gradient for generalized coordinate, i, from element m is

$$\frac{\partial \Pi_m}{\partial q_i} = \sum_{k=1}^{m} \frac{\partial \Pi_m}{\partial \bar{u}_k} \frac{\partial \bar{u}_k}{\partial q_i} \qquad (2)$$

by the chain rule. The partial derivatives $\frac{\partial \bar{u}_k}{\partial q_i}$ are given by Bradshaw [(1); pp. 22,23]. The partial derivatives, $\frac{\partial \Pi_m}{\partial \bar{u}_k}$, are computed numerically via the Gaussian quadrature. This quadrature is restated from Bradshaw [(1); p. 14]:

$$\frac{\partial \Pi_m}{\partial \bar{u}_k} = b \sum_{j=1}^{m} \sum_{i=1}^{n} A_i B_j \frac{\partial \Pi_m^*}{\partial \bar{u}_k} (x_i, y_j) \qquad (3)$$

The changes in the mathematical model which are necessary in order to make possible modeling nonlinear inelastic material behavior are contained in the formulation for internal energy density, Π^*, and the partial derivatives, $\frac{\partial \Pi^*}{\partial \bar{u}_k}$, k=1,2,3,4.

Internal energy density [4] at some point in an element is a function of the strain state at that location due to nodal displacements affecting the element. During the minimization process the values of stress, strain, and internal energy density at each Gauss point corresponding to the last equilibrium state are stored for reference during an iteration of the solution process. Consequently, the internal energy density at a Gauss point can be expressed as

$$\Pi^* = \Pi_1^* + \Delta\Pi^* \qquad (4)$$

where Π_1^* is the internal energy density at the last equilibrium configuration. $\Delta\Pi^*$ is the change in internal energy density resulting from a trial displacement configuration.

Referring to Fig. 3 it is seen that

$$\Pi_1^* = \int_0^{\varepsilon_1} \sigma \, d\varepsilon \tag{5}$$

and that

$$\Delta\Pi^* = \int_{\varepsilon_1}^{\varepsilon} \sigma \, d\varepsilon \tag{6}$$

For a linear stress-strain curve illustrated in Fig. 3, $\Delta\Pi^*$ can be written

$$\Delta\Pi^* = \frac{(\sigma + \sigma_1)(\varepsilon - \varepsilon_1)}{2} \tag{7}$$

and the stress can be written

$$\sigma = \sigma_1 + E(\varepsilon - \varepsilon_1) \tag{8}$$

where σ_1 and ε_1 are the stress and strain at a Gauss point for the last equilibrium state. The strain, ε, is defined by the trial displacement configuration and E is the slope of the stress-strain curve.

The piecewise linear, bilinear stress-strain relation, used in this model, is illustrated in Fig. 4 for a Gauss point location i. σ_{ti} , ε_{ti} and σ_{ci} , ε_{ci} are the yield coordinates in tension and compression respectively. σ_1 and ε_1 comprise the stress-strain state associated with the previous equilibrium state. E_1 and E_2 are the moduli of the elastic and inelastic portions of the bilinear constitutive function.

The stress-strain plane can be divided into three zones. These are illustrated in Fig. 4 . These zones are mathematically described by the following inequalities:

$$\begin{aligned} &\text{Zone 1} : \quad \varepsilon_c < \varepsilon < \varepsilon_t \\ &\text{Zone 2} : \quad \varepsilon \geq \varepsilon_t \\ &\text{Zone 3} : \quad \varepsilon \leq \varepsilon_c \end{aligned} \tag{9}$$

Both the $\sigma - \varepsilon$ coordinates and the $\sigma_1 - \varepsilon_1$ coordinates can exist in any

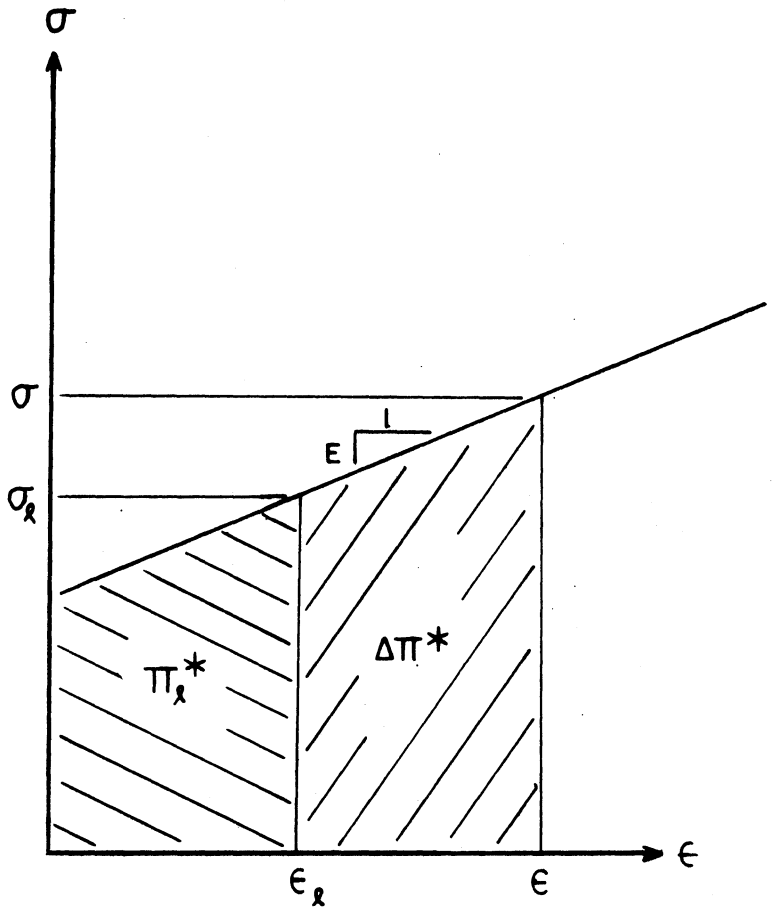

FIGURE 3 - STRAIN ENERGY DENSITY FOR LINEAR CONSTITUTIVE LAW

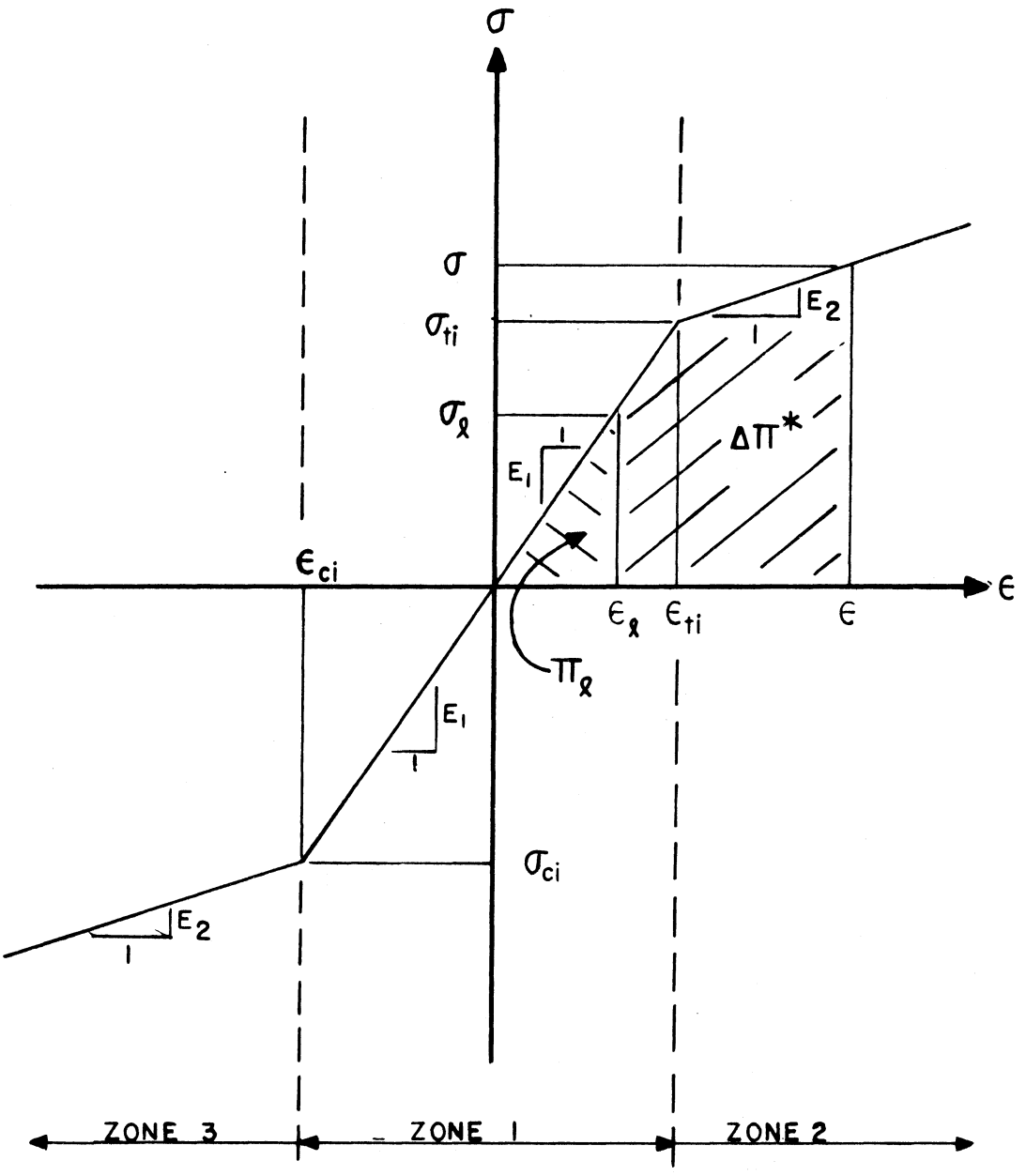

FIGURE 4 — BILINEAR CONSTITUTIVE LAW

of the three zones. Thus, nine possible combinations of the two pairs of coordinates can exist. Accordingly, nine formulations are possible for $\Delta\Pi^*$ and σ. The equations for $\Delta\Pi^*$ and σ take the form of Eqns. (7) and (8).

Unlike that for $\Delta\Pi^*$ and σ the formulation for the partial derivatives $\frac{\partial\Pi^*}{\partial\bar{u}_k}$ is simple. These derivatives can be written as:

$$\frac{\partial\Pi^*}{\partial\bar{u}_k} = \frac{\partial\Pi_1^*}{\partial\bar{u}_k} + \frac{\partial\Delta\Pi^*}{\partial\bar{u}_k} \qquad k= 1,2,3,4 \qquad (10)$$

However, the first term on the right-hand side of Eq. 10 is zero since Π_1^* is constant during an iteration of the solution process. Accordingly, Eq. 10 becomes

$$\frac{\partial\Pi^*}{\partial\bar{u}_k} = \frac{\partial\Delta\Pi^*}{\partial\bar{u}_k} \qquad k= 1,2,3,4 \qquad (11)$$

Referring to the segment of a linear stress-strain curve illustrated in Fig. 3 and to Eq. 7, it was shown by Holzer [4] that the partial derivative of $\Delta\Pi^*$ with respect to distortion components takes the following form for this special stress-strain function:

$$\frac{\partial\Delta\Pi^*}{\partial\bar{u}_k} = \sigma\,\frac{\partial\varepsilon}{\partial\bar{u}_k} \qquad k= 1,2,3,4 \qquad (12)$$

The bilinear stress-strain law used in this model is made up of linear segments. Eq. 12 is valid for any stress-strain state on this function.

The partial derivatives $\frac{\partial\varepsilon}{\partial\bar{u}_k}$ are given below in terms of derivatives of the interpolation functions and the nondimensionalized coordinate ξ.

$$\frac{\partial\varepsilon}{\partial\bar{u}_1} = \frac{\phi_1'}{L} \qquad (13)$$

$$\frac{\partial\varepsilon}{\partial\bar{u}_4} = \frac{\phi_4'}{L} \qquad (14)$$

$$\frac{\partial\varepsilon}{\partial\bar{u}_2} = \left(\frac{\phi_2'\bar{u}_2}{L} + \frac{\phi_3'\bar{u}_3}{L}\right)\frac{\phi_2'}{L} - \eta\,\frac{\phi_2''}{L} \qquad (15)$$

$$\frac{\partial\varepsilon}{\partial\bar{u}_3} = \left(\frac{\phi_2'\bar{u}_2}{L} + \frac{\phi_3'\bar{u}_3}{L}\right)\frac{\phi_3'}{L} - \eta\,\frac{\phi_3''}{L} \qquad (16)$$

The nondimensionalized coordinates, ξ and η, interpolation functions, ϕ_k, and their derivatives with respect to ξ are given by Bradshaw [(1); pp. 6,9,10].

Loading and unloading, expressed as movement of a stress-strain state along the stress-strain function and shifting of the function along its ε axis, take three forms:

1. Elastic loading and unloading

This mode of loading is characterized by movement of the stress-strain state along the elastic portion of the function in zone 1.

2. Inelastic loading

This is movement of the stress-strain state along the curve from zone 1 into zone 2 or zone 3.

3. Inelastic unloading

When a point of an element is unloaded after undergoing inelastic loading, the movement of the stress-strain state takes place parallel to the elastic portion of the function as illustrated in Fig. 5. The previous stress-strain state in zone 2 or 3 from which the unloading occurred becomes the yield coordinates delineating zone 2 or 3 respectively. The yield strain in zone 3 or 2 changes according to the elastic modulus and the yield stress in zone 3 or 2. The result is a shift in the constitutive function depicted by the dotted lines in Fig. 5.

The formulation for Π^* and $\frac{\partial \Pi^*}{\partial \bar{u}_k}$ is presented via flow charts in Figs. 6 and 7 [4].

Fig. 6 illustrates the initialization of yield coordinates and the initialization of stresses, strains and internal energy densities to zero before the solution process begins. During the solution process, the yield

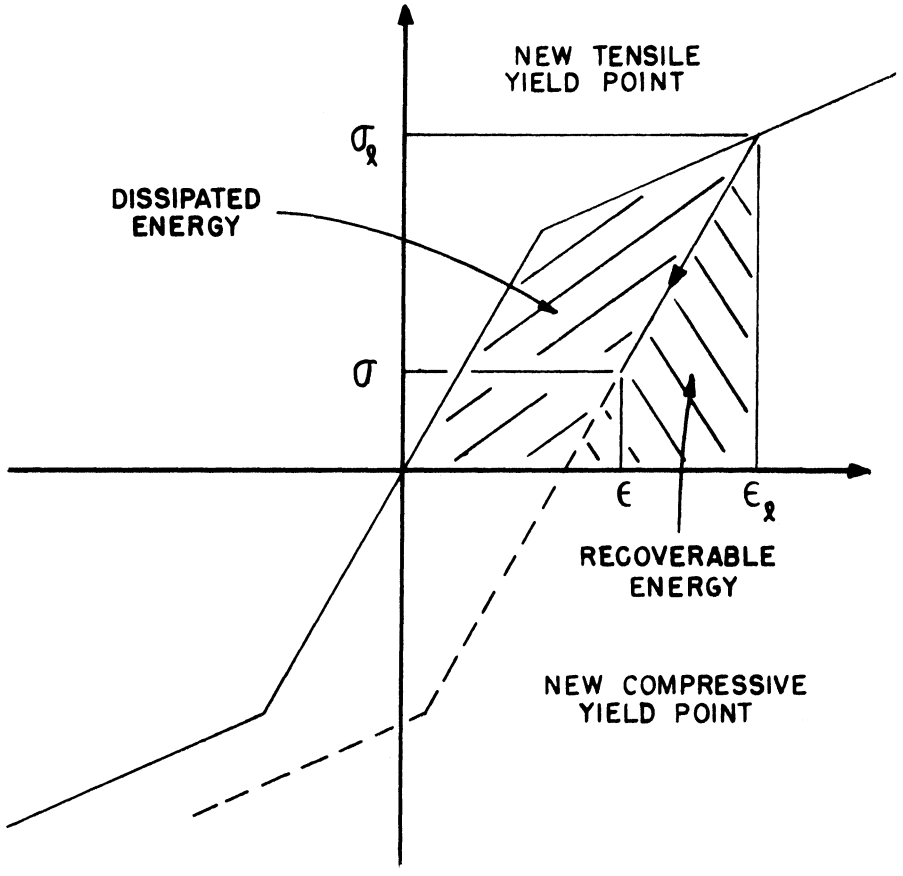

FIGURE 5 – INELASTIC UNLOADING

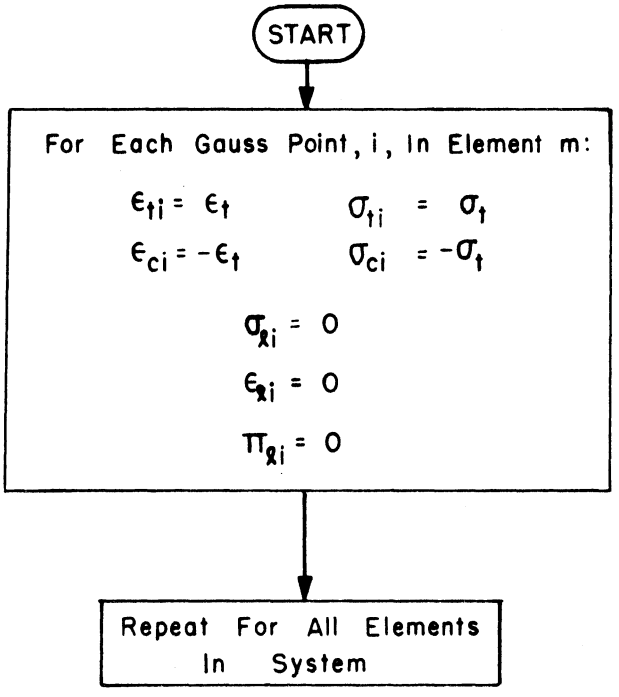

FIGURE 6 — INITIALIZATION OF GAUSS POINT [4] PARAMETERS

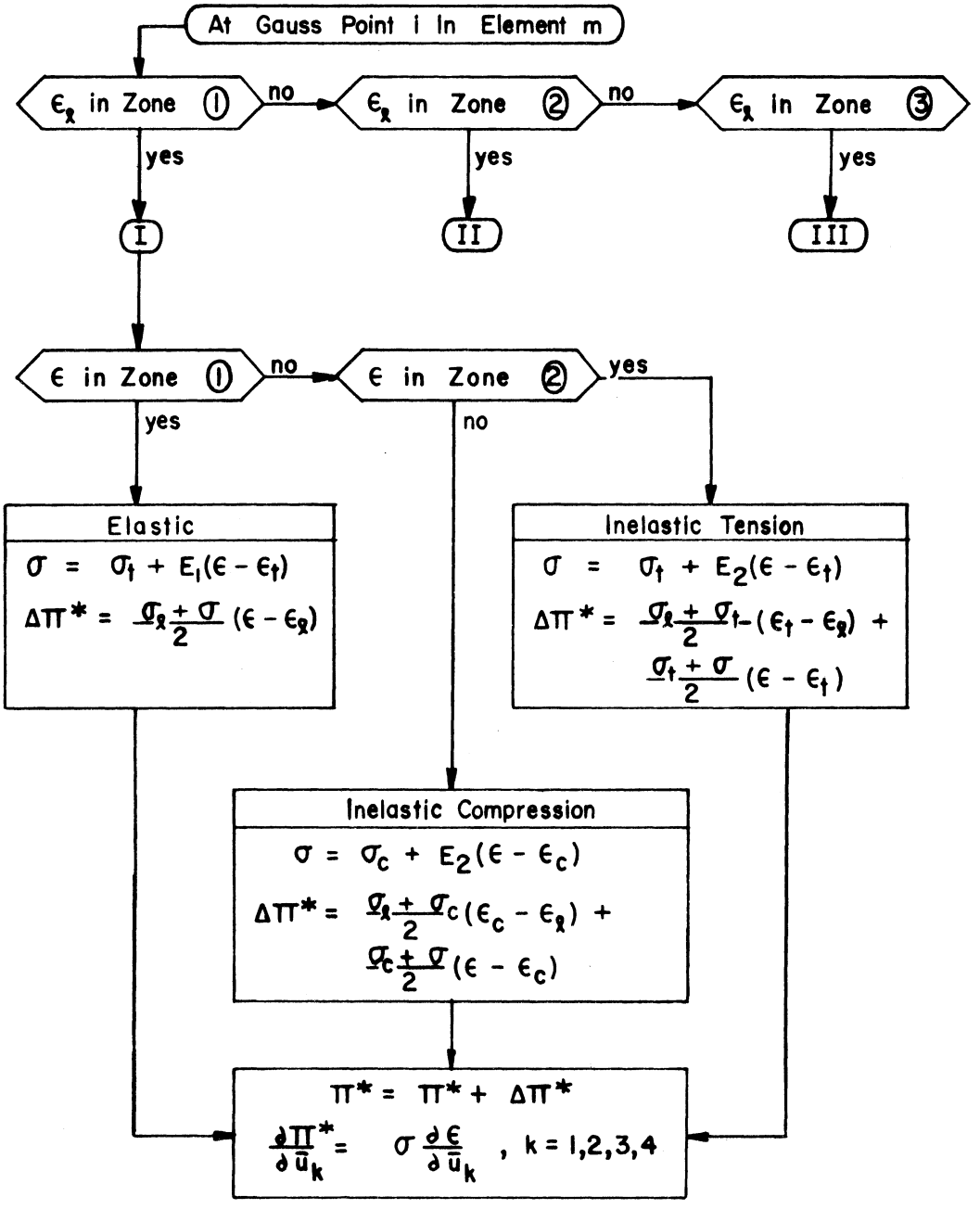

FIGURE 7 – NONLINEARLY INELASTIC INTERNAL ENERGY DENSITY [4]

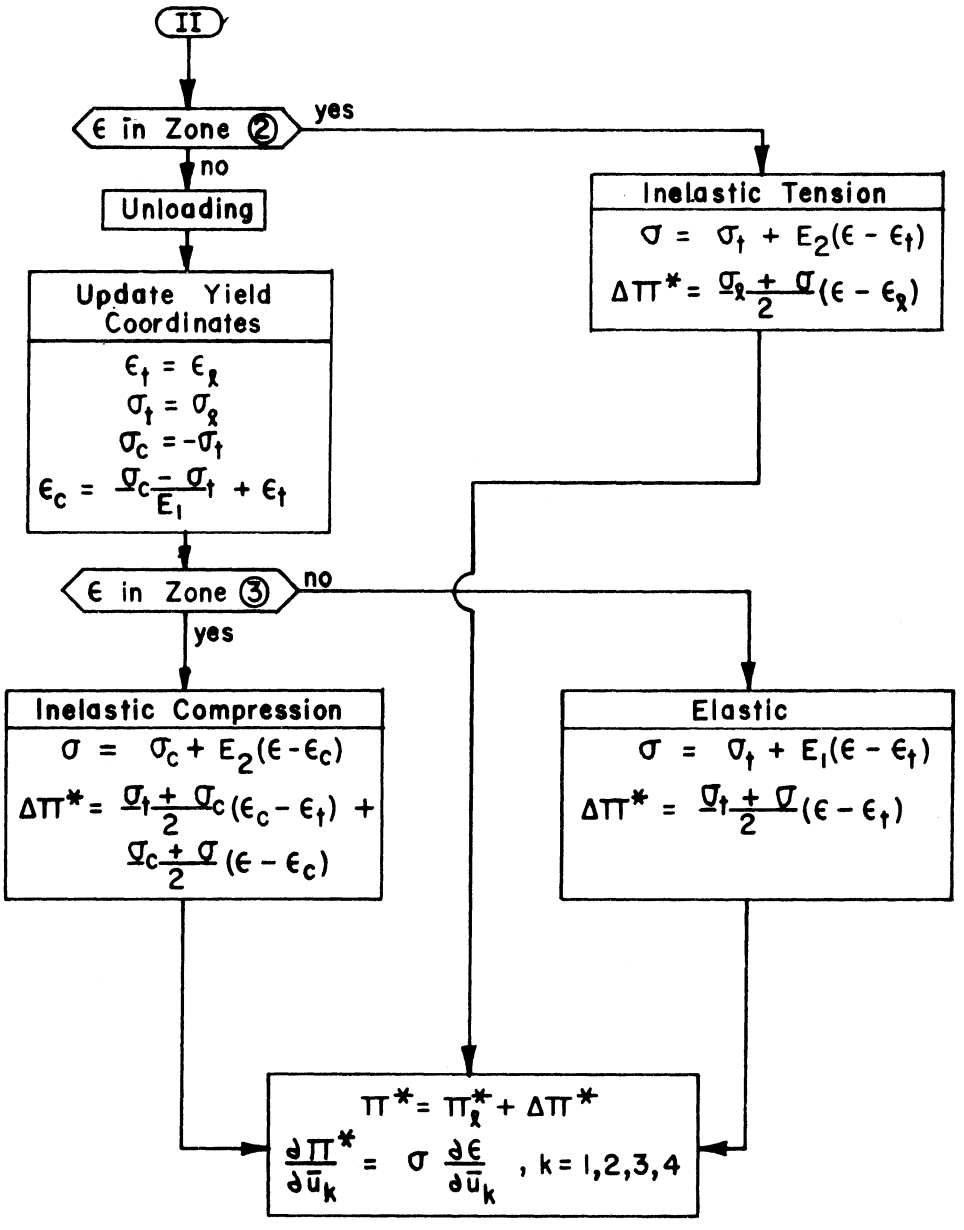

FIGURE 7 – CONTINUED

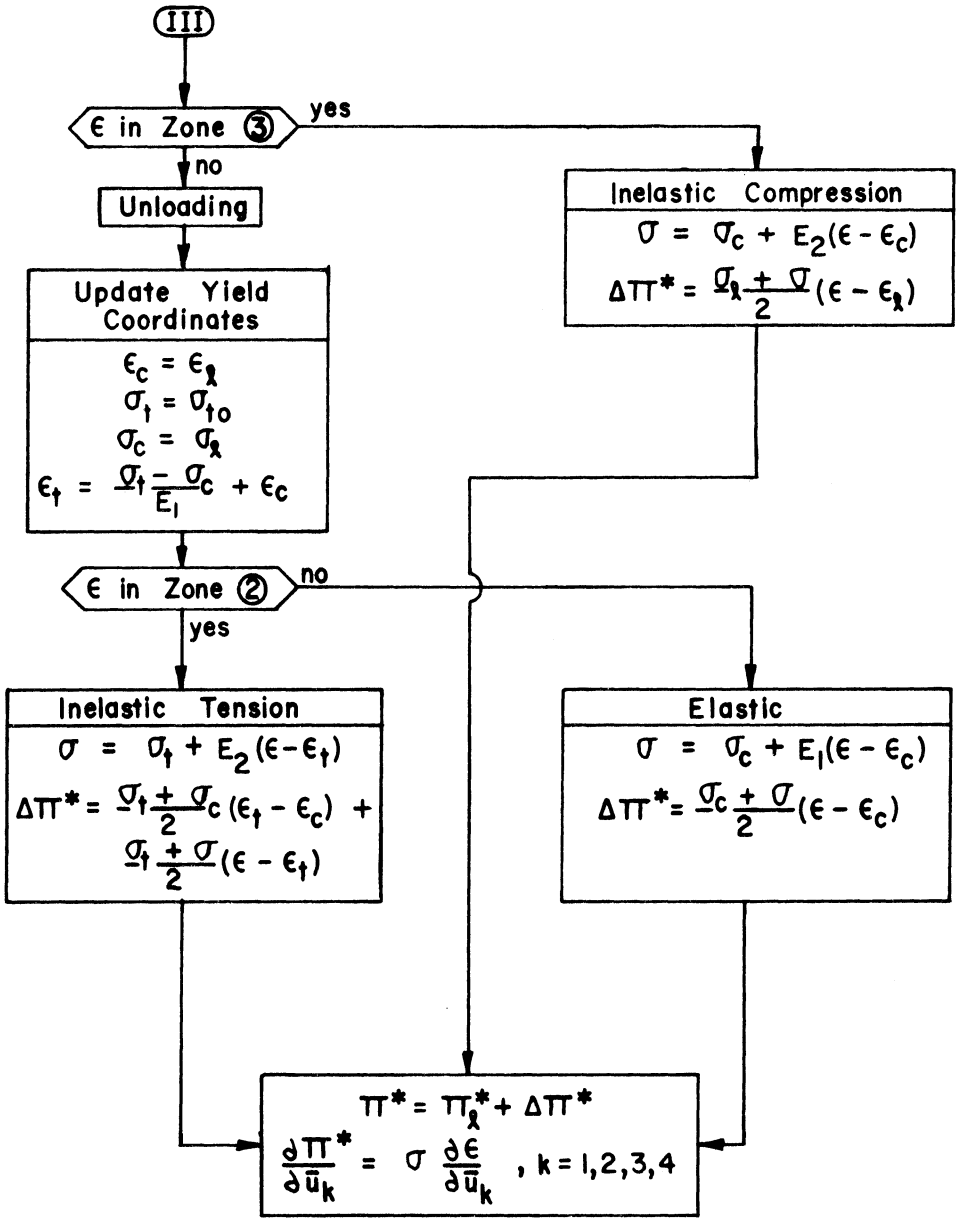

FIGURE 7 – CONTINUED

coordinates and values of stress, strain, and internal energy density for the last equilibrium state at a Gauss point must be retrieved from storage. From these values and the trial strain, the stress, and internal energy density can be computed.

CHAPTER III

Model Validation

An investigation was conducted in order to determine the ability of the model to predict inelastic beam-column behavior.

Demonstration problems are presented in two groups. The first group consists of problems whose solutions are compared to those obtained by means of existing mathematical models. The second group consists of two problems which demonstrate the validity of two features of this model.

Comparison Group

1. Eccentrically loaded, inelastic beam-column

This problem was chosen to test the ability of the model to predict the fundamental equilibrium path of an inelastic beam-column.

Timoshenko and Gere [5] present a solution for the equilibrium path of a simply supported beam-column with an eccentric axial load, which was initially investigated by Karman [6]. The constitutive law is identical to that used by Karman.

Timoshenko presents plots of the magnitude of the axial load versus mid-column displacement for several eccentricities in nondimensionalized form. The axial load, P, is nondimensionalized with respect to the Euler buckling load, P_e, for a simply supported column while the mid-column displacement Δ_c is nondimensionalized with respect to the depth of the column in the plane of displacement, h.

A beam-column identical in geometry and support conditions to that described by Timoshenko was analyzed using the computer program described previously.

The constitutive law used by Karman was obtained from uniaxial compression tests on steel specimens [6]. Accordingly, the stress-strain curve is nonlinear and continuous. In order to use the model, this nonlinear constitutive law must be approximated by a bilinear relationship. The best approximation was chosen as follows:

Initial compressive yield stress (σ_{ci}): 45 ksi

Elastic modulus (E_1): 30860 ksi

Inelastic modulus (E_2): 1625 ksi

Support and loading conditions are illustrated in Fig. 8. The eccentricity of the axial load, P, is .005h.

Initially, a four-element assemblage and a 2 X 2 Gauss rule were employed to represent the beam-column. First attempts at using the computer program to generate an equilibrium path revealed that the solution process would converge to displacement configurations for load steps until the yield strain was reached in the outer fiber of an element. Further loading with the same load step size (load increment) resulted in failure by the solution process to converge to meaningful equilibrium configurations. Three schemes were tried in order to extend the equilibrium path.

1. Reducing the magnitude of the load increment.
2. Increasing the Gauss rule to 7 X 7.
3. Increasing the number of elements.

Increasing the Gauss rule and the number of elements had very little effect on convergence.

It was found that reducing the load increment allowed the solution process to converge for load steps above first yielding. As inelastic deformation proceeded, the maximum allowable load increment decreased

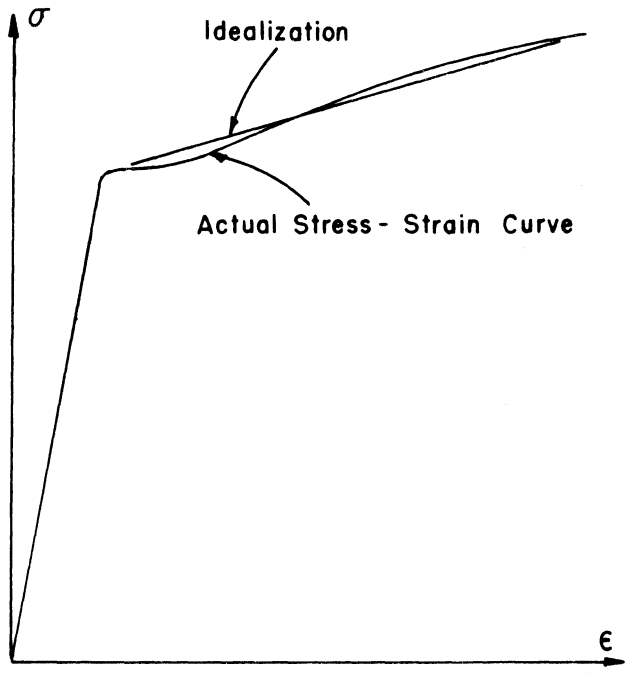

TYPICAL STRESS - STRAIN IDEALIZATION

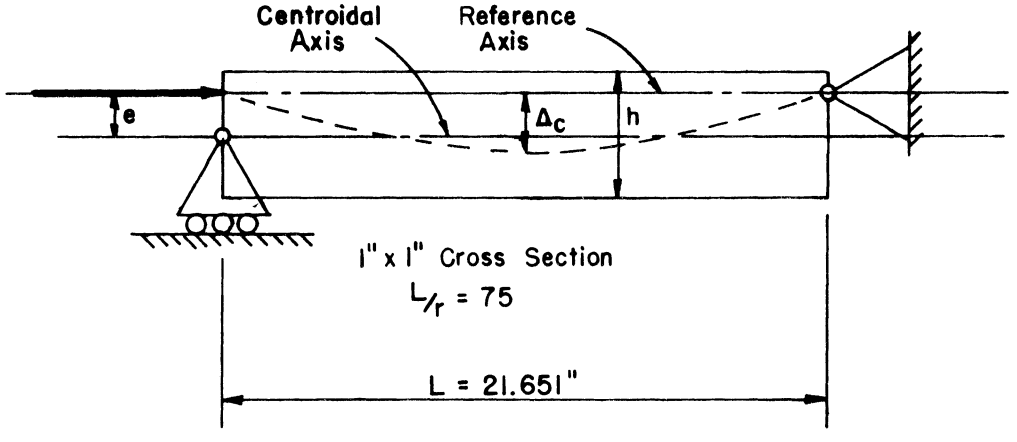

ECCENTRICALLY LOADED BEAM - COLUMN

FIGURE 8

further. The maximum load for which an equilibrium configuration was solved is 40266 pounds. The load increment required for convergence for load steps 40250 through 40266 pounds was 2 pounds, or .005% of the 40250 pound load level. This was considered a practical limit to refining the load increment.

A plot of the equilibrium path provided by the model is presented in Fig. 9. Inspection of Fig. 9 indicates that the small load increments, necessary to allow convergence of the solution process, can be associated with the equilibrium path approaching a limit state.

2. Inelastic beam-column

A computer program was written at the Fritz Laboratory at Lehigh University [7] to implement a mathematical formulation for the analysis of a nonlinearly inelastic beam-column. Characteristics of the model are summarized below.

a. Admissible geometry: The beam-column must be prismatic and simply supported at its ends.

b. Admissible constitutive law: The stress-strain curve must be elastic-plastic.

c. Admissible loading: Loading consists of an axial load and a concentrated transverse load applied at mid-span. The axial load may be concentric or eccentric. The magnitude of the axial load is fixed during an analysis while the magnitude of the transverse load is increased by increments.

d. Solution process: Curvature of the centroid at mid-span is incremented during the solution process. For each mid-span curvature step, the curvature at the ends of the beam-column, the

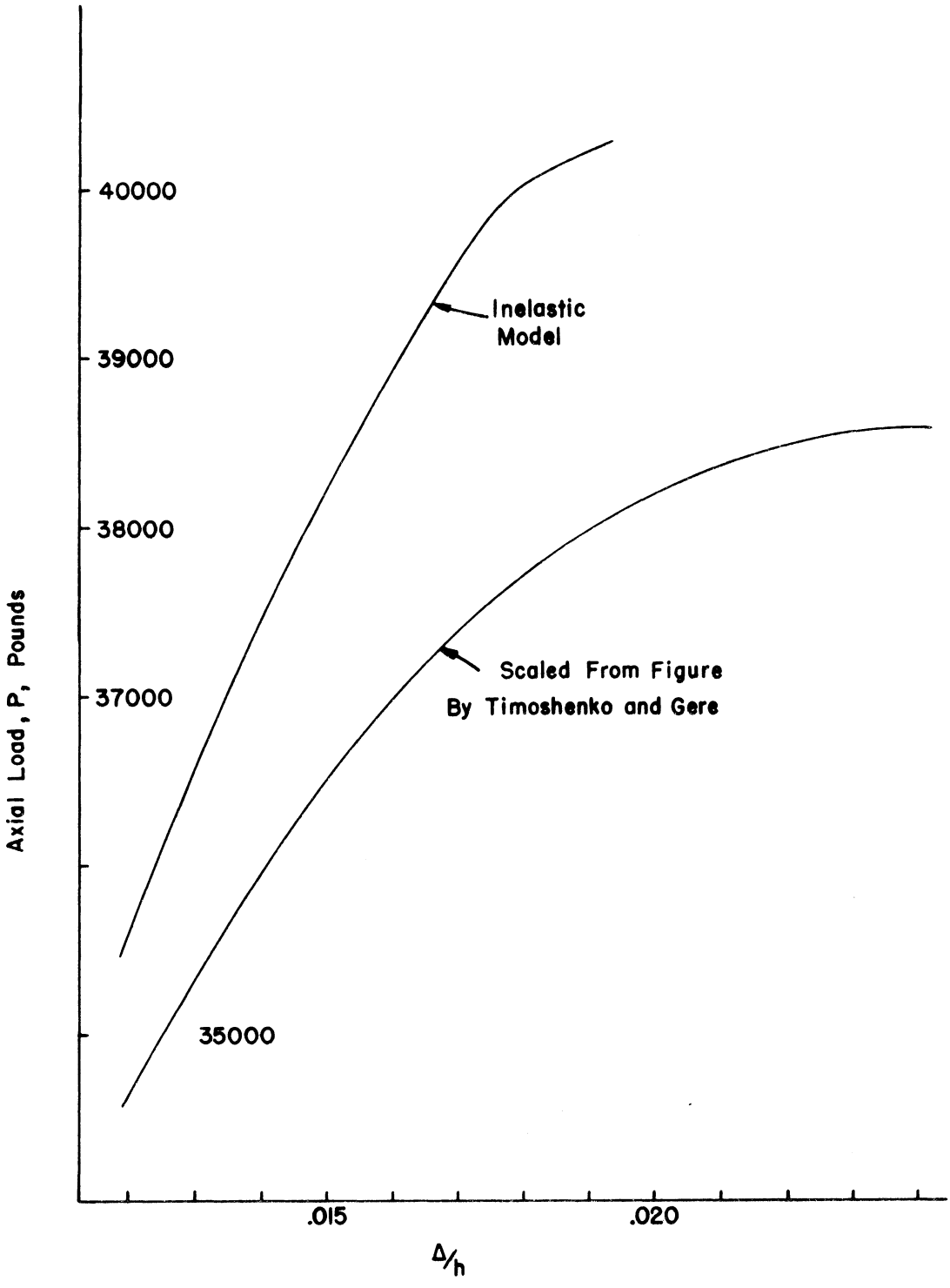

FIGURE 9 – ECCENTRICALLY LOADED INELASTIC COLUMN

displacement at the mid-span, and the transverse load at mid-span required for equilibrium are computed.

The results of an analysis with this model take two forms. In the first case, the beam-column exhibits a limit state. The Lehigh formulation and program produce stable equilibrium configurations up to the limit state, then unstable ones after the limit state. These unstable states are marked by increasing displacement with decreasing mid-span load.

In the second case, the beam-column never becomes unstable. For this case the Lehigh program continues the solution process until the load at mid-span corresponds to the ultimate moment that can be developed at mid-span. This ultimate moment is that moment corresponding to a plastic hinge at mid-span. At this point the solution process ceases. When plotted, this equilibrium path looks similar to that associated with a limit state although it is not associated with a limit state.

Two beam-column problems were investigated for which the model and the Lehigh program were used to carry out the analyses. In the first problem, the loading conditions were such that a limit state resulted. The loads in the second problem were chosen so that the system would not attain a limit state but remain stable for very large displacements.

The beam-column structure investigated is 120 inches in length with a 2 inch square cross section. The elastic-plastic constitutive law is defined by an elastic modulus of 29 million psi, and a yield stress equal to 40000 psi.

For the first problem, two element meshes were used with the model, one with four and one with eight elements. For both meshes a 7 X 7 Gauss rule was used in each element. The concentric axial load was

16000 pounds. A transverse concentrated load was applied in load steps at mid-span. The beam-column is illustrated in Fig. 10.

In Fig. 11, equilibrium paths for both the model and the Lehigh program are presented; they are plots of the mid-span load versus mid-span displacement.

In order to approach the transverse load at the limit state, the size of the load increment was reduced until, in the neighborhood of the limit state, the load increment was equal to one pound or .1% of the mid-span load considered to approximate the limit load.

The difference in the predicted limit load between the two models was less than one percent when a four element representation was used. The eight element mesh produced an equilibrium path nearly identical to that by the Lehigh model. It is also noted that as the element mesh becomes finer, from 4 to 8 elements, the equilibrium path produced by the model approaches that of the Lehigh program.

The second problem chosen for comparison with the Lehigh formulation is identical to the first except that the magnitude of the fixed axial load is 1000 pounds. Two element meshes were used with the model, one with four and the other with eight elements. A 7 X 7 Gauss rule was used.

As in the first problem, the transverse load was incremented from zero.

As illustrated in Fig. 12, the results of the model indicated that no limit state occurred. Stable equilibrium states were predicted by the model for very large mid-span displacements. The curve produced by the Lehigh program follows closely that of the model up to the neighborhood

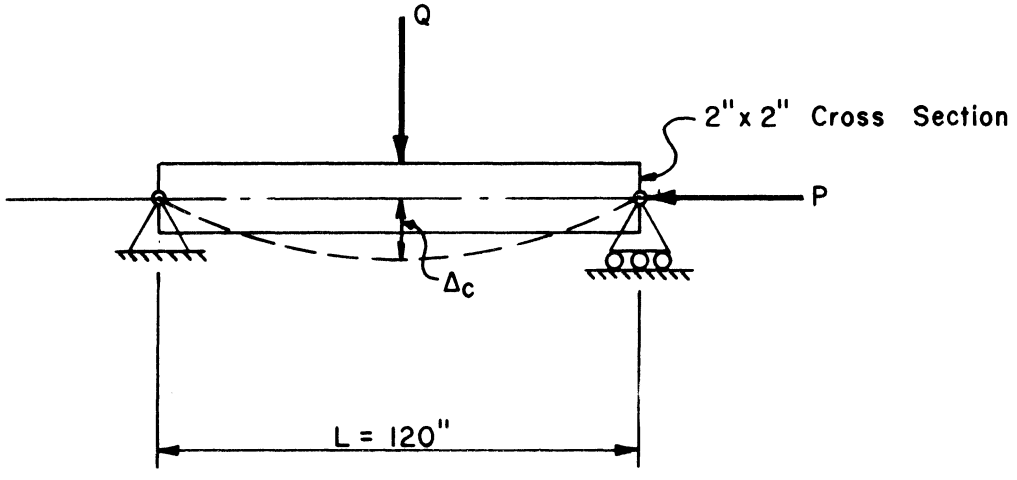

FIGURE 10 – BEAM-COLUMN WITH CONCENTRIC AXIAL LOAD, FOR COMPARISON WITH THE LEHIGH MODEL

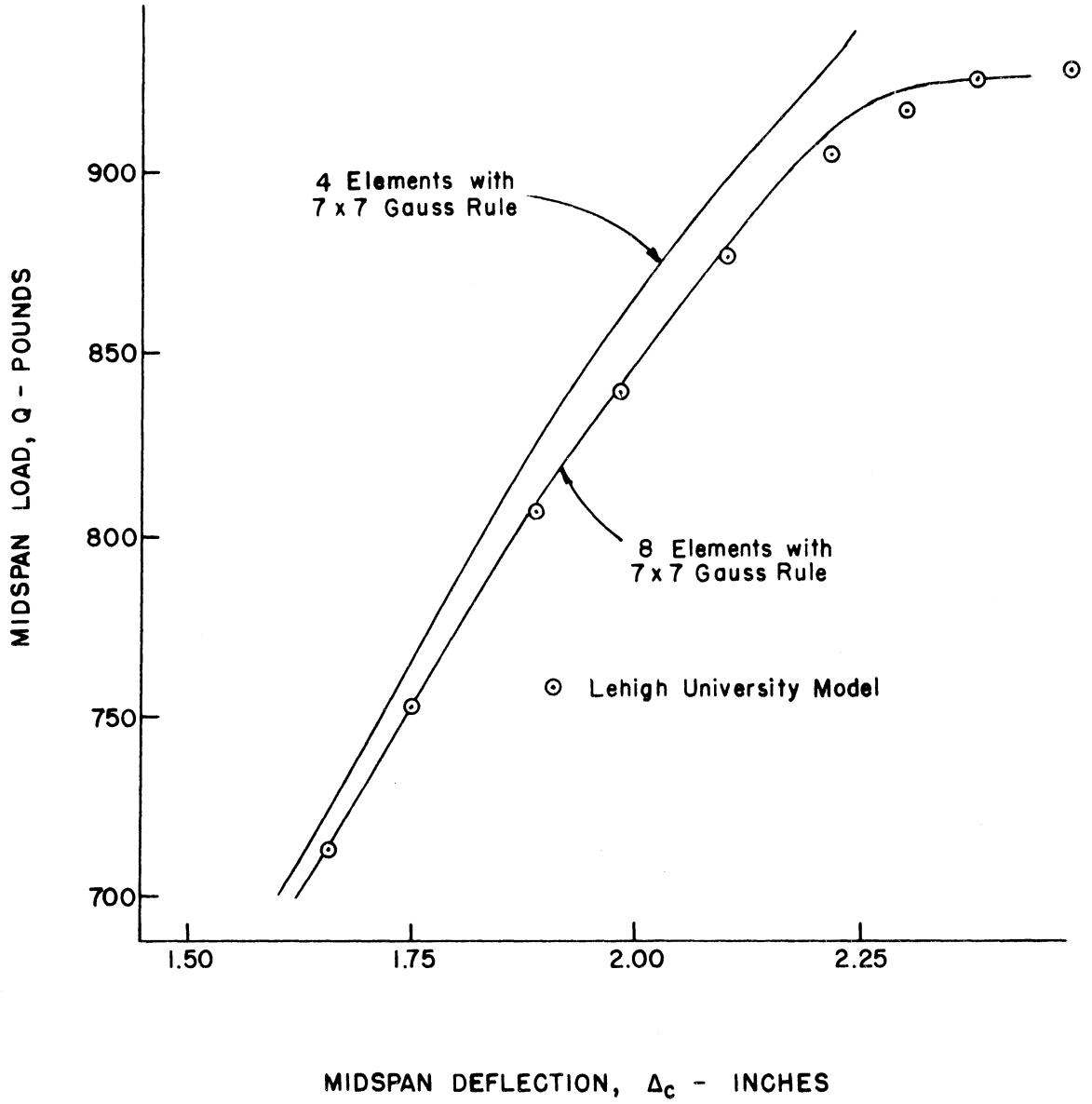

FIGURE 11 - TRANSVERSE MIDSPAN LOAD vs MIDSPAN DEFLECTION FOR ELASTIC-PLASTIC BEAM-COLUMN WITH 16000 POUND CONCENTRIC AXIAL LOAD

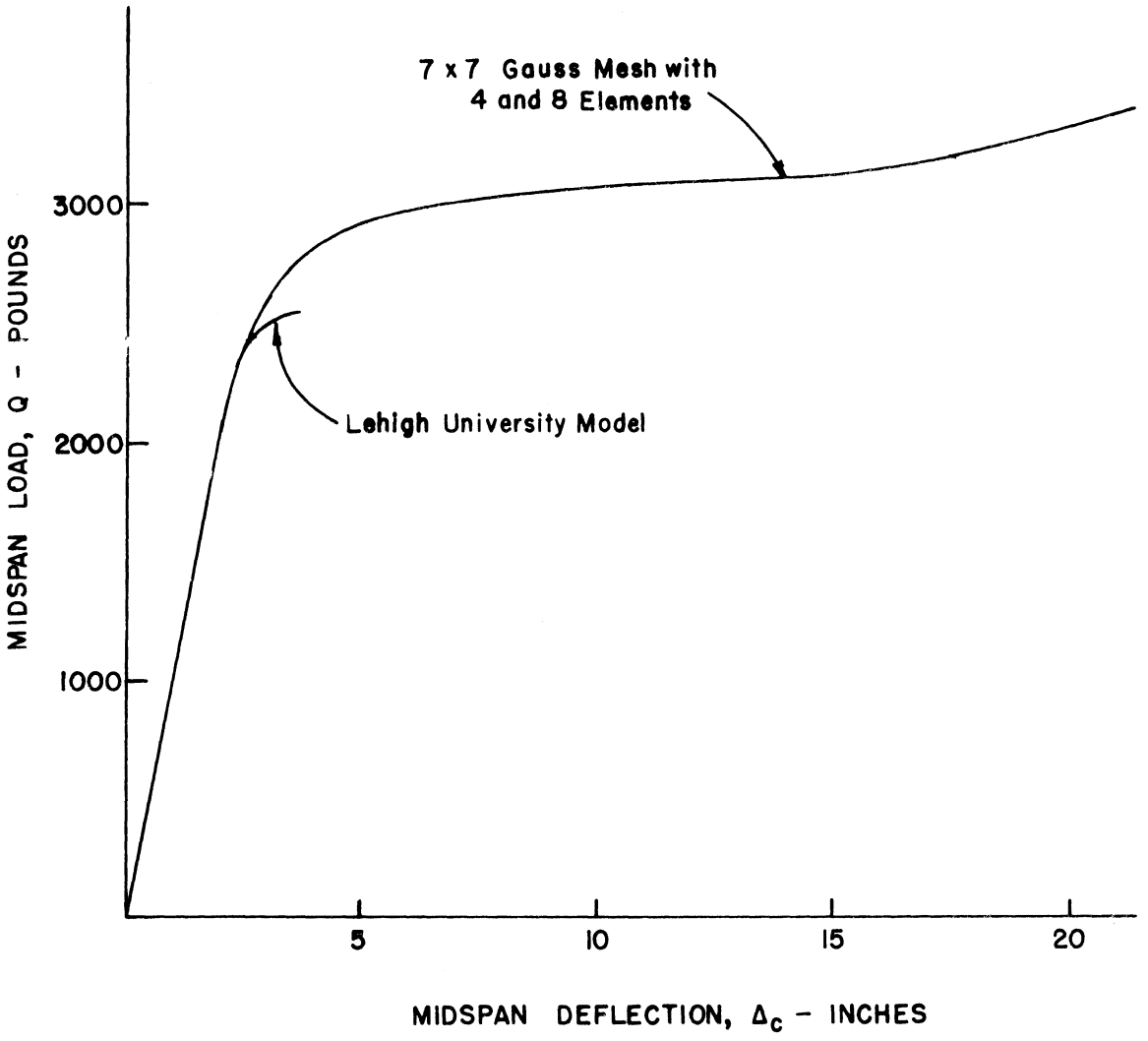

FIGURE 12 — TRANSVERSE MIDSPAN LOAD vs MIDSPAN DEFLECTION FOR ELASTIC-PLASTIC BEAM-COLUMN WITH 1000 POUND CONCENTRIC AXIAL LOAD

of the mid-span load corresponding to a theoretical plastic hinge at mid-span. Near the ultimate load the slope of the Lehigh curve changes rapidly and becomes nearly zero at the ultimate load. At this point, as mentioned previously, the Lehigh program ceases. The Lehigh curve is forced to resemble a limit state at the ultimate load.

The plot produced by this model extends somewhat above the ultimate load computed by the Lehigh program, then its slope decreases and the plot reveals stable equilibrium configurations for very large displacements.

3. Elastica problem

This comparison problem is designed to investigate the performance of the model when only geometric nonlinearities are involved. Timoshenko and Gere [5] present a solution to the "elastica problem", which is that of determining equilibrium configurations above the bifurcation point for a perfectly elastic concentrically loaded column. These configurations exist only with large displacements; thus, a geometrically nonlinear model is required. Since the constitutive law is perfectly elastic, the use of the model to solve for equilibrium states would exercise only the geometric nonlinearities contained in the model.

Nondimensionalized results for a free standing beam-column are given by Timoshenko [5] . This free standing column is illustrated in Fig. 13. The nondimensionalized axial load is expressed as the ratio of axial load to the Euler buckling load, $\frac{P}{P_e}$.

Displacements giv en by Timoshenko, both transverse and parallel to the undeformed axis, are nondimensionalized with respect to the undeformed length of the beam-column. A plot of these results is presented in Fig. 14.

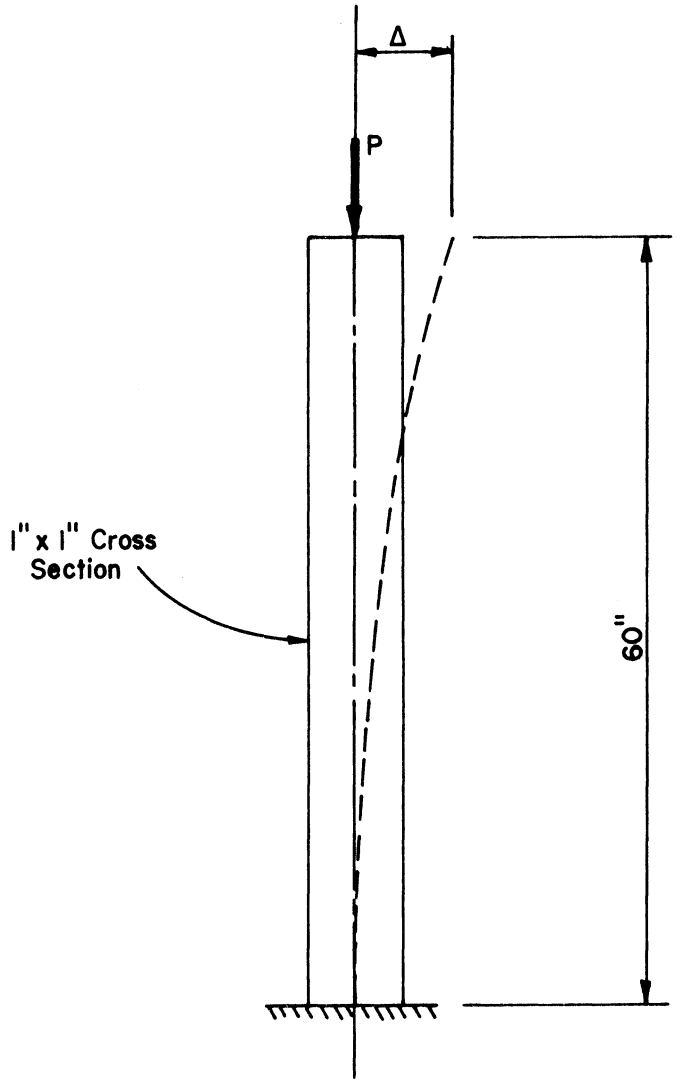

FIGURE 13 – FREE STANDING, PERFECTLY ELASTIC BEAM-COLUMN

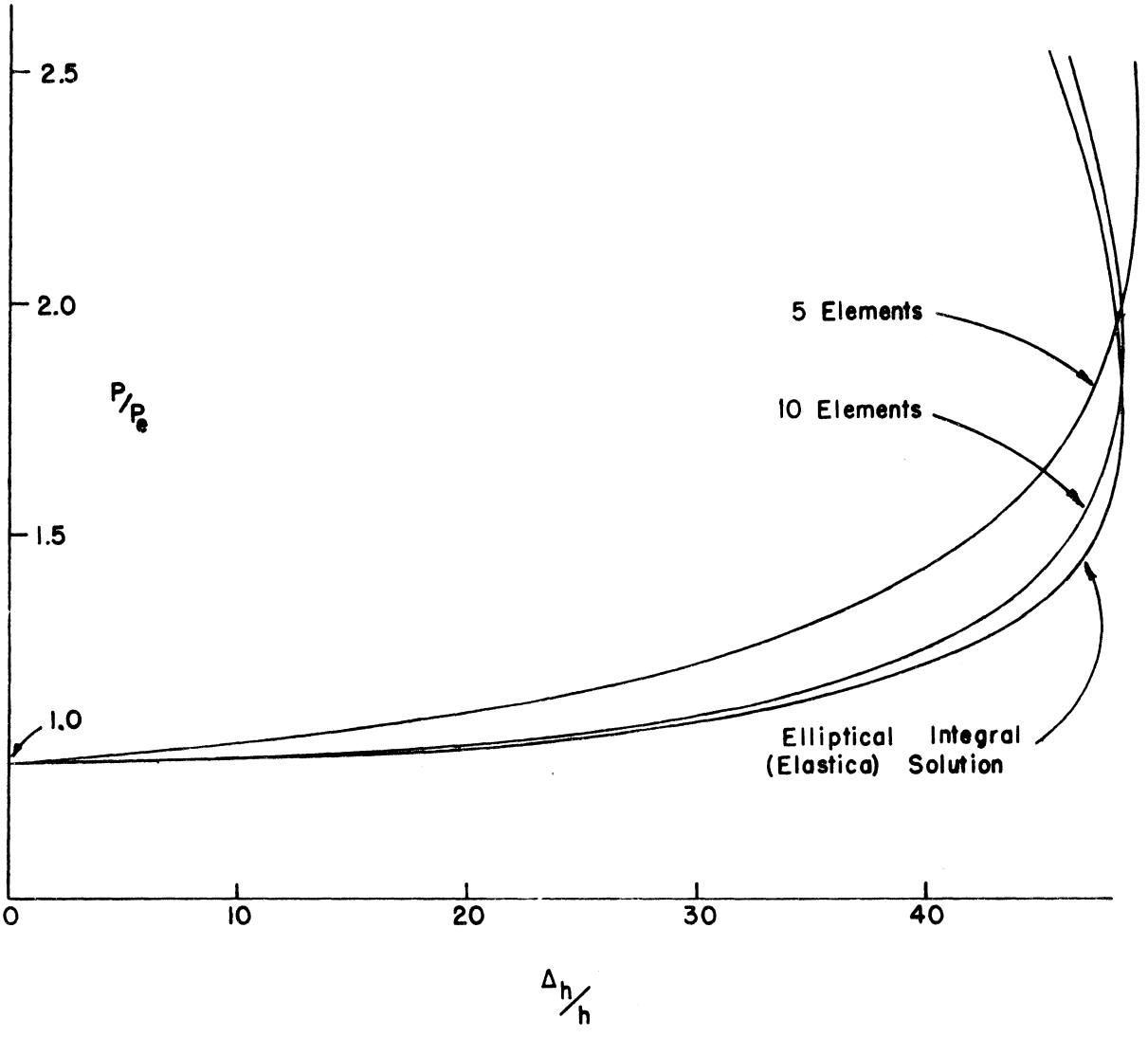

FIGURE 14 - PERFECTLY ELASTIC FREE STANDING COLUMN

Analysis by the model was performed using a beam-column with a one inch square cross section and a length of 60 inches. The constitutive law was perfectly elastic with an elastic modulus equal to 30 million psi. This was done by specifying a very large yield stress. Two element meshes were used, one with five elements and one with ten elements. A 5 X 2 Gauss mesh was used in each element since it is shown in Ref. 2 that a 5 X 2 Gauss rule yields exactly the element internal energy.

The end constraints were those of a free-standing beam-column; free at the loaded end and fixed at the opposite end.

The loading consisted of a monotonically increasing concentric axial load.

Two schemes were tried in the attempt to obtain equilibrium configurations above the bifurcation point. The first scheme consisted of beginning with a first load step equal to 10% of the Euler load from zero, then increasing monotonically the load beyond the Euler load. There resulted no bifurcation point. Deformation at load steps far greater than the Euler load remained purely axial.

The second scheme consisted of beginning the analysis with a configuration of very small transverse displacements. This configuration was completely arbitrary and did not constitute a known equilibrium configuration. However, the solution process of the model converged to an equilibrium configuration for the first load step which was one-half pound above the Euler load. This equilibrium state exhibited transverse displacements as well as displacements parallel to the undeformed axis.

Further loading yielded the equilibrium paths illustrated in Fig. 14.

As the element mesh was refined, from five to ten elements, the equilibrium paths produced by the model approached that of Timoshenko's continuum model. The finite element results are everywhere stiffer than those of the continuum model.

SPECIAL PROBLEMS

1. Shifting reference axis

A variation of the Lehigh comparison problem presented earlier was investigated in order to observe the effect of shifting the reference axis on the response prediction. Instead of a centroidal axial load, a 16000 pound axial load is applied at the reference axis which is shifted up a distance a = .5 inches from the centroid. Also applied at the reference axis, at each end of the beam-column, are moments equal to Pa shown in Fig. 15. This loading is externally statically equivalent to a 16000 pound load at the centroid. The geometry of the beam-column is identical to that for the Lehigh comparison problems. An eight element mesh was used.

The analysis results for the 16000 pound centroidal load are presented in Fig. 11. The results for the shifted reference axis are presented in Fig. 16. It is seen that the shift resulted in little change in the response from that in Fig. 11. Strains at mid-span are presented in Table 1.

Also examined was the effect of shifting the reference axis on the convergence rate or number of minimization iterations required to reach an equilibrium configuration for each load step. No significant change was observed.

2. Cyclic Loading

An investigation was conducted in order to demonstrate the ability of the model to simulate inelastic loading beyond the yield strain, unloading from the load-deformation state due to inelastic loading, and reloading

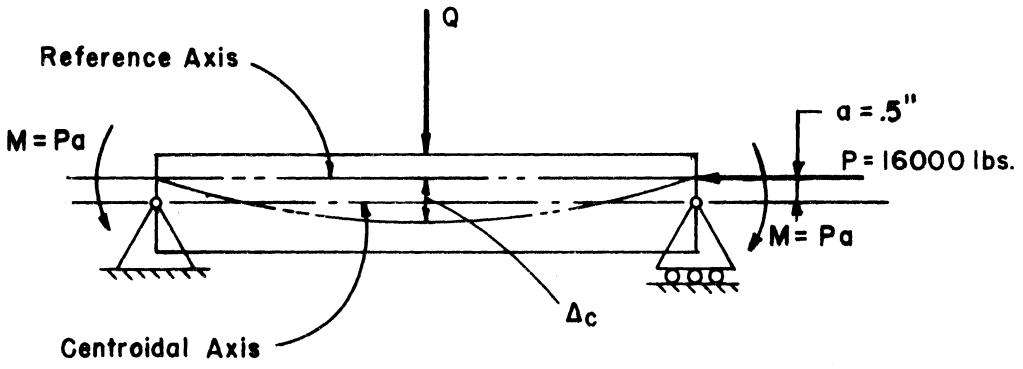

FIGURE 15 – SHIFTED REFERENCE AXIS

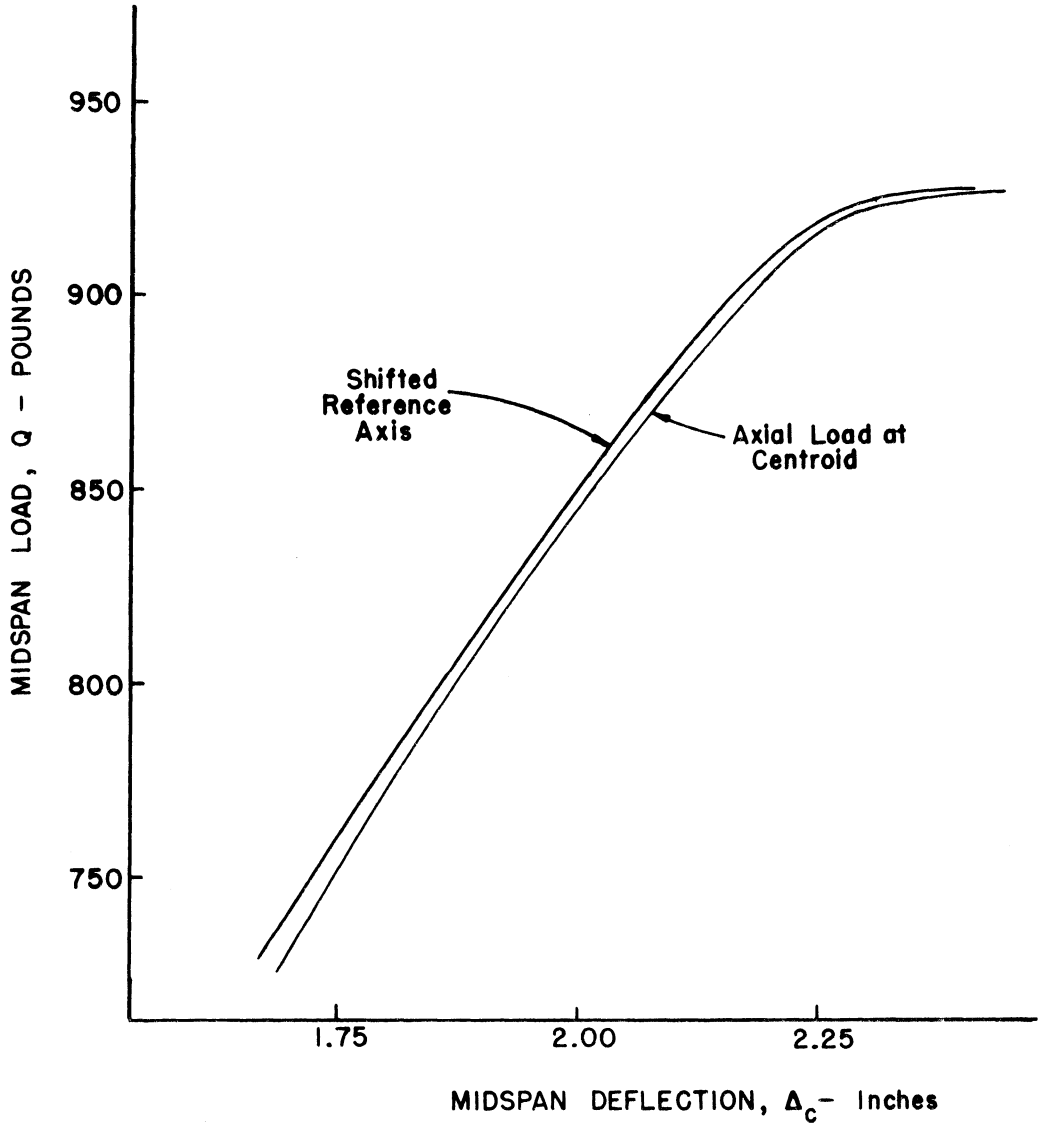

FIGURE 16 — BEAM-COLUMN WITH SHIFTED REFERENCE AXIS

TABLE 1 - Strains for Lehigh Beam-Column With 16000 Lb. Axial Load

	Ref. Axis at Centroid		Ref. Axis .5 Inch Above Centroid	
Q	ε at Top	ε at Bottom	ε at Top	ε at Bottom
400	-.0008123	.0005340	-.0008119	.0005336
800	-.001501	.001209	-.001498	.001207
900	-.001764	.001439	-.001761	.001436
915	-.001831	.001495	-.001819	.001486
922	-.001913	.001556	-.001887	.001337

from an unstressed but deformed state resulting from unloading.

The structure used for this demonstration is a single beam-column element fixed at one end and free at the other. An axial load, P, was applied at the centroid at the free end in such a manner that the modes of loading behavior described above were created. This structure is shown in Fig. 17. The yield stress is 40000 psi; the elastic modulus is 29 million psi; and inelastic modulus is 2.9 million psi. The cross section of the element is one inch by one inch so that the load and stress are equal in magnitude.

The loading sequence took the following form:

1. P was applied in tension from 0 to 40000 pounds, the yield load: elastic loading
2. P was further increased from 40000 pounds to 48000 pounds: inelastic loading
3. P was then decreased from 48000 pounds to 0: unloading
4. P was then increased in compression from zero to -40000 pounds, the yield load: elastic reloading
5. P was then further increased from -40000 pounds to -48000 pounds: inelastic reloading
6. Finally, P was allowed to return to zero: unloading

The amounts of tensile loading and unloading and compressive reloading and unloading are equal in magnitude. The resulting equilibrium path should be a closed polygon beginning and ending at the origin. These results are plotted in Fig. 18.

The analysis by the model produced exactly the same equilibrium path as that in Fig. 18.

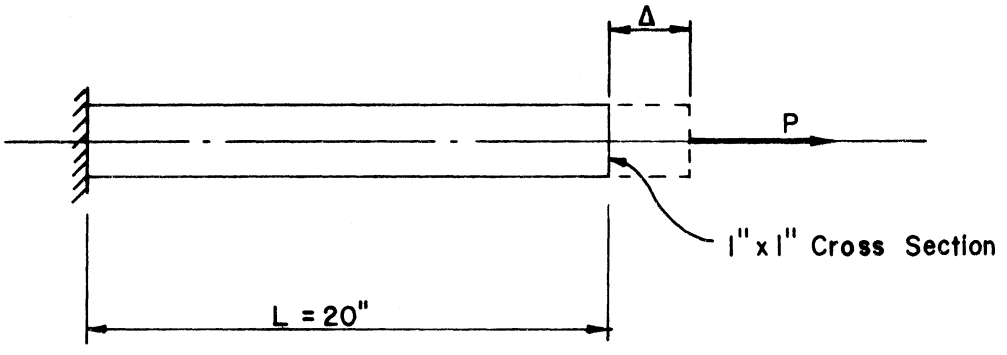

FIGURE 17 - UNIAXIALLY LOADED BAR

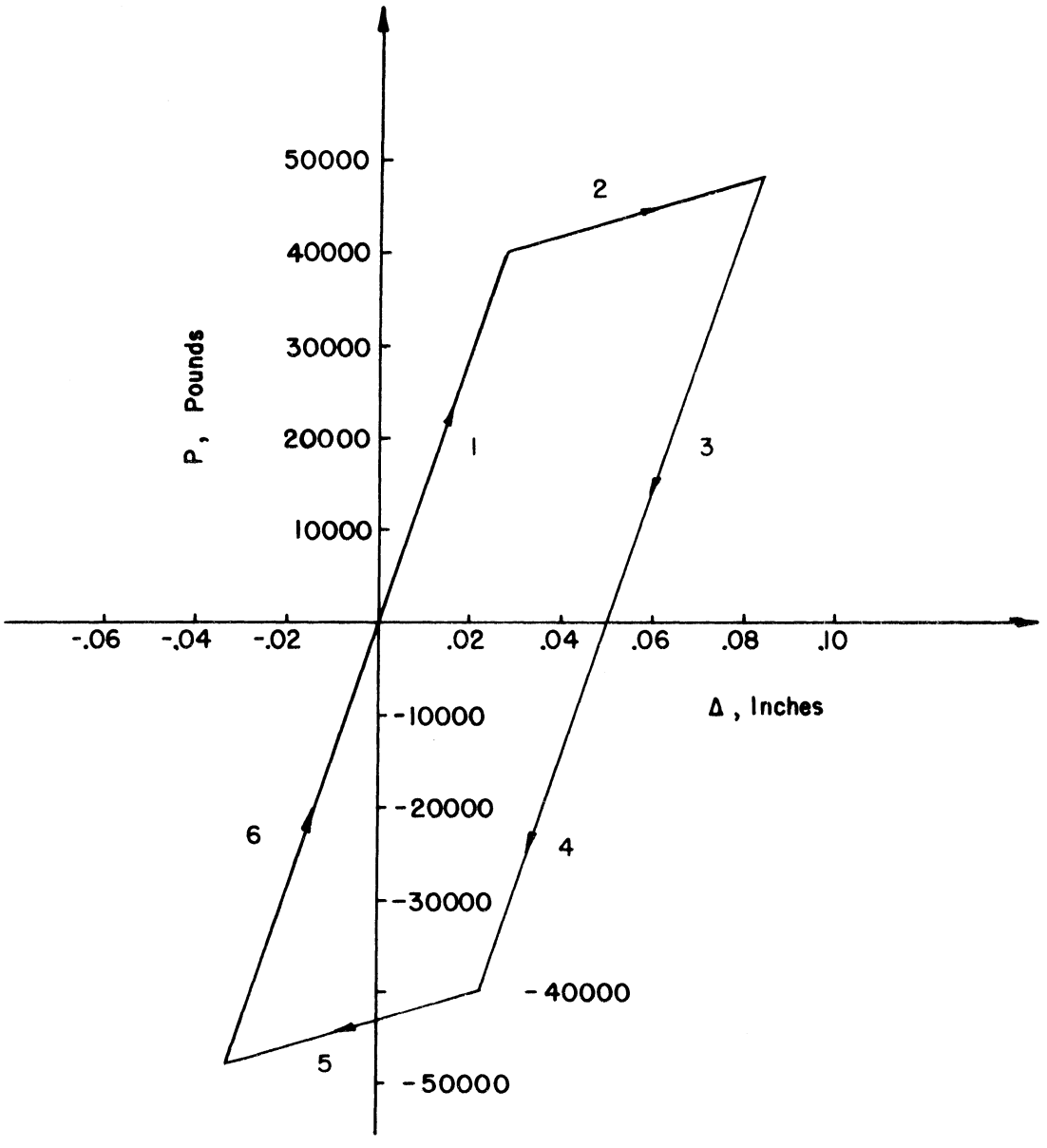

FIGURE 18 – CYCLIC LOADING

CHAPTER IV

Observations and Notes

Limit State

Two criteria were used to examine the performance of the model in predicting the existence of a limit state. The equilibrium path was examined, looking for a steadily decreasing slope tending toward a slope of zero. Also, the displacement and load at the possible limit state were compared to those produced by the corresponding model. During the solution by the model for an equilibrium path, some indication of an approaching unstable state was sought. This indication might be in the form of the necessity that the load step be reduced or that the number of elements be increased to allow further solution for the equilibrium path.

Inspection of the equilibrium path obtained with this model for an inelastic beam-column, which was compared to that obtained by Timoshenko and Gere (Fig. 9) revealed that its slope steadily decreases up to the load corresponding to attainment of the yield stress in the outer fibers of the beam-column. At this load there is a marked change in slope of the path. Beyond this load the slope again decreases but not at as high a rate as before first yielding. The slope at the point on the path where the solution was halted was not equal to zero. The shape of the equilibrium path is not conclusive evidence that a limit state has been reached. The agreement between load and displacement at the limit state indicated by Timoshenko's curve and the last equilibrium configuration produced by this model is not close. This may be due to the difference in constitutive laws.

As noted in Chapter Three, the solution for the equilibrium path was halted when the largest load step which would allow convergence to a stable equilibrium configuration had decreased to 2 pounds, or .005% of the load at that level. This indicated that stable equilibrium states still existed for higher axial loads. The use of larger load steps would only result in the solution process indicating that no minimum could be found to the energy function within the limitation on the number of iterations allowed for searching. It is felt that at some load in the immediate neighborhood of this last one solved, the solution process would not have been able to converge in any number of iterations, or that no stable state could be found at all. Hence, the last equilibrium state solved is considered to be in the immediate neighborhood of the limit point.

Examination of the equilibrium path obtained for the Lehigh beam-column with a 16000 pound axial load (Fig. 11) reveals very close agreement with the Lehigh data. Also, the path attains a slope of nearly zero. These facts indicate that the model can predict attainment of a limit state.

Comparison with the Lehigh model produced closer agreement than that obtained in the comparison with the inelastic eccentrically loaded beam-column of Timoshenko and Gere. This is true since an exact duplication of stress-strain functions was possible for the Lehigh comparison.

Effect of Element Mesh Refinement

Zienkiewicz [8] states " . . . if true equilibrium requires an absolute minimum of the total potential energy an approximate finite element solution by displacement approach will always provide an approximate

minimum which is greater than the correct one." He further states " . . . the approximate solution always underestimates the value of strain energy . . .". Zienkiewicz is speaking of elastic, conservative systems. It follows that displacements produced by a finite element model should be smaller in magnitude than those produced by a continuum model.

The free standing column used to compare the model with a continuum model possessed a perfectly elastic constitutive law; so it represented a conservative system. The constitutive law used for both Lehigh comparison problems was inelastic. However, since these beam-columns were never unloaded, there was no opportunity for the system to become nonconservative. Since no strain energy was dissipated, the model, for the elastica and Lehigh comparisons, should produce displacements which are smaller in magnitude than those of the elliptic integral model or the Lehigh model since both of these are continuum models.

Inspection of Figs. 11 and 14 indicate that this expectation was born out. In both comparisons the results of the model indicated stiffer responses than those of the continuum models.

More important, though, is the effect of increasing the number of elements in a given structure. During the above mentioned comparison investigations, the number of elements for both structures were doubled and the equilibrium paths redeveloped. In both cases the equilibrium paths indicated less stiff responses for the finer element meshes but still stiffer than the results of the continuum models (Figs. 11 and 14). This is as expected.

In the case of the Lehigh comparison, refining the element mesh resulted in completely different types of limit state response. The four

element model indicated a stiff, almost linear ascent to an abrupt limit state. The eight element representation produced a smooth approach which became steadily less stiff up to the limit state.

Effect of Shifting Reference Axis

A feature of this model is that the reference axis, from which the relative displacements of an element are taken, can be located anywhere in the depth of the element. This is discussed by Holzer, et al [2]. If the feature is valid, the model must yield the same equilibrium paths and strain distributions for analyses conducted with the reference axis located at various locations in the element.

As was presented in Chapter Three, this was done for the Lehigh beam-column with axial load equal to 16000 pounds. The equilibrium paths generated by the two models are nearly the same. An examination of the strains tabulated in Chapter Three reveals that up through a mid-span load equal to 900 pounds, or about 27 pounds from the limit load, the strains produced by the two analyses are nearly identical.

From this single test it appears that the "floatable" reference axis feature is performing, at least from a practical point of view.

Ability to Model Dissipative Unloading

Examination of the equilibrium path for the cyclically loaded bar indicates that for the simple loading scheme, the model is capable of modeling dissipative unloading and reloading.

Magnitude of Load Step

While studying a single degree of freedom of a simple structure under a simple load configuration, it was found that it was often necessary to reduce the magnitude of the load step as the generation of the equilibrium

path progressed.

This was necessary to insure that the number of iterations required by the minimization algorithm to converge to an equilibrium configuration did not exceed a limit which is chosen by the user. Since the user cannot foresee the load level at which load steps will need to be reduced, he must try sets of loads until a set is found which will allow solution for the entire equilibrium path. It is most desirable that a feature be added to the model whereby the model can automatically reduce the load steps as the equilibrium path is generated.

SUMMARY

Tests conducted to investigate the performance of this model indicate the following:

1. The model can predict the existence of a limit state.

2. The model can predict the existence of stable equilibrium states accompanied by large displacements for simple structures and load configurations.

3. Responses produced by the model are sensitive to the element mesh refinement and load step size.

4. The floating reference axis feature of the model appears to perform nearly as intended but not perfectly.

5. The formulation can model equilibrium paths corresponding to uniaxial loading, unloading, and reloading of a bar which involves dissipation of strain energy.

BIBLIOGRAPHY

1. Bradshaw, J.C., "Nonlinear Analysis of Plane Frames", Thesis, Virginia Polytechnic Institute & State University, Blacksburg, Va., May 1975.

2. Holzer, S.M., Melosh, R.J., Barker, R.M., and Somers, Jr. A.E., "SINGER: A Computer Code for General Analysis of Two-Dimensional Concrete Structures", AFWL-TR-74-228, Vol. 1, Air Force Weapons Laboratory, Kirtland Air Force Base, N.M., May 1975.

3. Holzer, S.M., Somers, Jr. A.E., and Bradshaw, J.C., "Reliability Study of SINGER", AFWL-TR- , Vol. 1, Air Force Weapons Laboratory, Kirtland Air Force Base, N.M., in print.

4. Holzer, S.M., unpublished notes.

5. Timoshenko, S.P., and Gere, J.M., Theory of Elastic Stability, McGraw-Hill Book Company, New York, 1961.

6. Karman, T.V., Collected Works of Theodore Von Karman, Vol. 1, Butterworths Scientific Publications, London, 1956.

7. Iyengar, S., and Chen, W.F., "Computer Program for an Inelastic Beam-Column Element", Fritz Engineering Laboratory Report No. 331.7, May 1970, Fritz Engineering Laboratory, Lehigh University, Pa.

8. Zienkiewicz, O.C., The Finite Element Method in Engineering Science, McGraw-Hill Book Company, London, 1971.

9. Fletcher, R., and Powell, M.J.D., "A Rapidly Convergent Descent Method for Minimization", Computer Journal, Vol. 6, Iss. 2, 1963, pp. 163-168.

APPENDIX A

Changes in the Computer Program

The changes necessary to achieve the modeling of inelastic behavior are twofold.

1. Additions are made to the main program such that at the completion of the solution process for an equilibrium configuration, the stress, strain, and internal energy density at each Gauss point location in the system are stored for future retrieval.

2. The formulation for strain energy density and its partial derivatives with respect to the distortion components was removed from Subroutine STNG [(1); Appendix B]. In Subroutine STNG, in Bradshaw's program, the Gaussian quadrature is executed to compute strain energy and its gradients for an element. Also, it is used on special command to evaluate strains at the extreme corners of an element.

The formulation which was removed from Subroutine STNG was replaced by Subroutine STENDN. STENDN computes the internal energy density and its gradients at a Gauss point location for inelastic behavior. These parameters are used by the ramainder of STNG to complete the Gaussian quadrature for internal energy and its gradients for an element.

A flow chart of Subroutine STNG by Bradshaw is given in Fig. A. The portion of that routine which has been removed and replaced by STENDN is cross-hatched in Fig. A.

Subroutine STENDN executes the formulation presented via flow charts in Figs. 6 and 7.

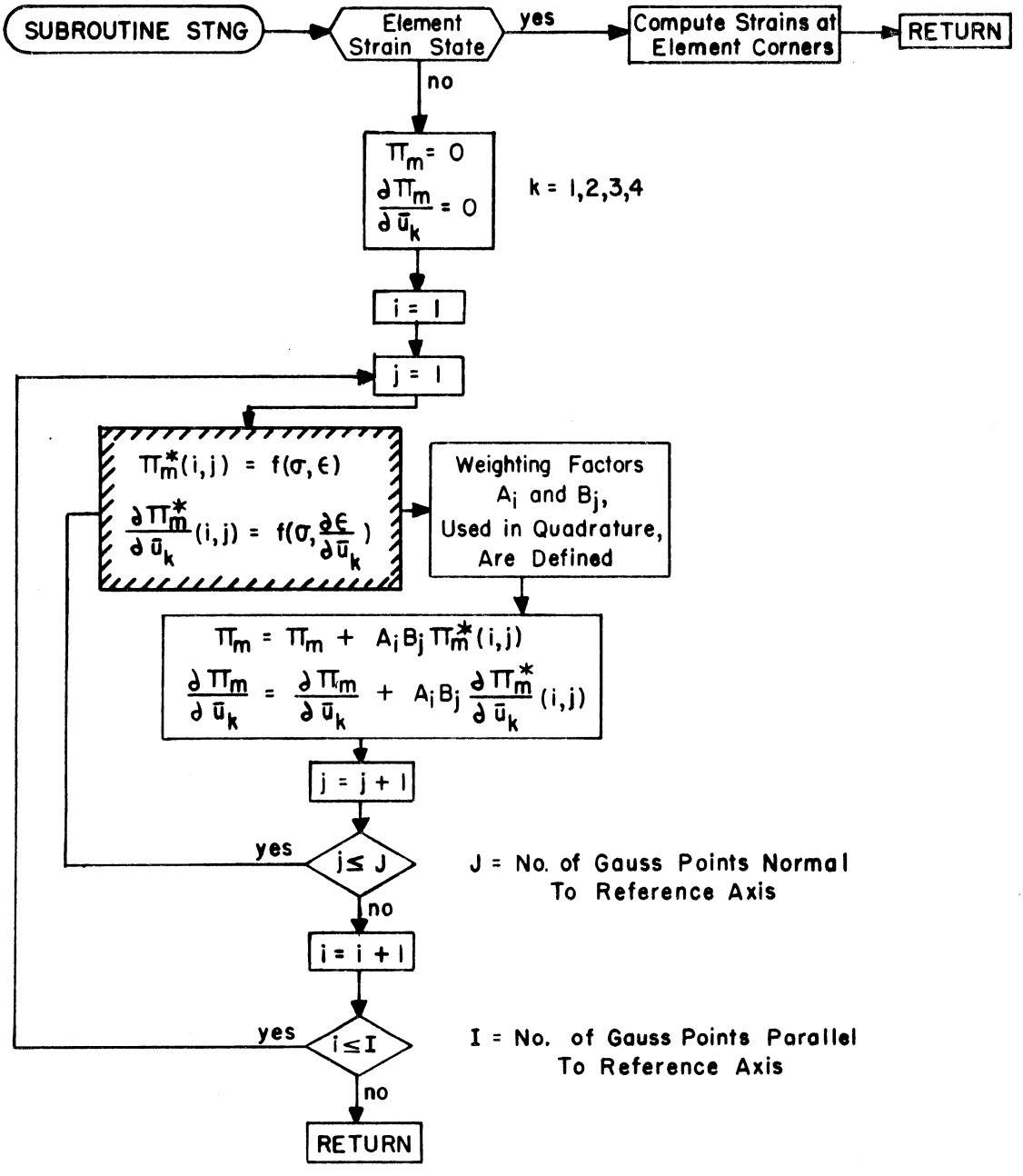

FIGURE A — SUBROUTINE STNG [1]

Attention Patron:

The one-page vita has been removed

from the scanned document

ANALYSIS OF NONLINEAR BEAM-COLUMNS

by

Ronald B. Shiflett

(ABSTRACT)

A finite element model of a beam-column featuring geometrical nonlinearities and a nonlinearly elastic constitutive law has previously been developed and tested.

The model was subsequently extended to include an inelastic constitutive law.

An investigation was conducted to test the performance of the inelastic model. The problems used to test the model include the following:

1. Inelastic, geometrically nonlinear beam-column.
2. Elastic, geometrically nonlinear beam-column.
3. Inelastic bar under cyclic, uniaxial loading.

The solutions provided by the inelastic model were compared to those produced by already existing beam-column models.

The model provides reliable solutions to elastic and inelastic beam-columns. Specifically, it is useful for studying beam-columns which exhibit limit states.